COSMIC-2 Radio Occultation Constellation-First Results

W.S. Schreiner[1], J.P. Weiss[1], R.A. Anthes[1], J. Braun[1], V. Chu[2], J. Fong[2], D. Hunt[1], Y.-H. Kuo[1], T. Meehan[3] W. Serafino[4] J. Sjoberg[1], S. Sokolovskiy[1], E. Talaat[4], T.K. Wee[1], Z. Zeng[1]

[1]COSMIC Program, University Corporation for Atmospheric Research

[2]National Space Organization, Taiwan

[3]Jet Propulsion Laboratory, NASA

[4]NESDIS, NOAA

Corresponding author: Richard Anthes (anthes@ucar.edu)

Key Points:

- First operational tropical constellation of radio occultation (RO) satellites is collecting atmospheric bending angles and refractivity profiles of unprecedented quality
- Six advanced Global Navigation Satellite System (GNSS) RO receivers provide up to 5,000 high signal-to-noise ratio (SNR) profiles per day in the tropics
- First publicly available RO data from GLONASS
- Initial data show high accuracy and precision, deep penetration into lower troposphere, and ability to detect super-refraction
- COSMIC-2 data are freely available to the scientific community in near real time for operational forecasting and scientific research

Abstract

Initial data from the Formosa Satellite-7/Constellation Observing System for Meteorology Ionosphere and Climate (FORMOSAT-7/COSMIC-2, hereafter C2), a recently launched Equatorial constellation of six satellites carrying advanced radio occultation receivers, exhibit high signal-to-noise ratio, precision, and accuracy, and the ability to provide high-vertical-resolution information on temperature and water vapor in the challenging tropical atmosphere. After an initial calibration/validation phase, over 100,000 soundings of bending angles and refractivity that passed quality control in October 2019 are compared with independent data, including radiosondes, model forecasts, and analyses. The comparisons show that C2 data meet expectations of high accuracy, precision, and capability to detect super-refraction. When fully operational, the C2 satellites are expected to produce ~5,000 soundings per day, providing freely available observations that will enable improved forecasts of weather, including tropical cyclones, and weather, space weather, and climate research.

Plain Language Summary

This paper describes an initial quality assessment of satellite observations from a recently launched (25 June 2019) constellation of six satellites that orbit Earth over the tropics. The data, obtained using a relatively new technique called radio occultation, provide information of unprecedented quality on the temperature and water vapor in the tropics. These observations,

which are freely available to forecasters and researchers worldwide, will be useful in improving forecasts of weather, including tropical cyclones, and supporting weather and climate research.

1. Overview of COSMIC-2 Mission

COSMIC-2 (C2), a Taiwan-U.S. six-satellite mission, was launched on 25 June 2019 (Anthes and Schreiner, 2019). Each satellite carries an advanced Tri-GNSS (Global Navigation Satellite System) Radio Occultation (RO) System instrument (TGRS) developed by NASA's Jet Propulsion Laboratory (Tien et al., 2011). The TGRS includes a high-gain beam-forming RO antenna, and is achieving the highest signal-to-noise ratio (SNR) of RO measurements to date (>2500 V/V in a 1 Hz band). When fully operational, the C2 satellites are expected to produce 5,000 soundings per day in the tropics and subtropics, providing high-vertical-resolution information on the temperature and water vapor structure that will enable improved global weather forecasts and a unique, freely available data set that will support weather and climate research. C2 will also provide data arcs of total electron content (TEC) and vertical profiles of electron density in the ionosphere to support space weather operations and research. C2 is an operational follow-on to the FORMOSAT-3/COSMIC (hereafter COSMIC) research mission launched in 2006 (Anthes, 2011; Ho et al., 2019), and is a successful example of a research to operations transition. This paper takes a first look at the quality of the C2 RO data by comparing them with other independent data sets, including operational radiosondes, short-term operational model forecasts and MERRA-2 reanalyses (Gelaro et al., 2017). Most of the comparisons use over 100,000 C2 profiles from October 2019, after an initial calibration/validation phase.

The C2 satellites will be deployed into six evenly spaced circular orbital planes of 24° inclination at an altitude of about 550 km. In addition to the TGRS, each satellite carries two space weather instruments, the Ion Velocity Meter (IVM) and the Radio Frequency Beacon (RFB). The IVM measures in-situ ion temperature, velocity, and density. The RFB is a transmitter that enables measurements of TEC and ionospheric scintillation by ground receivers. These instruments will contribute to the forecasting of space weather events, monitoring and prediction of scintillation (e.g. Equatorial plasma bubbles and sporadic E-clouds), and understanding of the coupling between the lower and upper atmosphere. Results from these instruments will be presented in the future.

A network of 10 downlink ground stations, located in Australia, Brazil, French Polynesia, Ghana, Guam, Hawaii, Honduras, Kuwait, Mauritius, and Taiwan, receives data and routes them to Taiwan and the U.S. for processing. This network enables C2 data to be made available in near real time (more than half the observations processed within 30 minutes) for use in numerical weather prediction (NWP) and space weather prediction. The data are freely available and may be obtained from the COSMIC Data Analysis and Archive Center (www.cosmic.ucar.edu).

2. Initial Results

2.1. Signal to noise ratio (SNR) and other characteristics of C2 RO soundings

C2 is producing higher SNR values than any previous RO mission, owing to the advanced TGRS receiver and high-gain antenna. Early results indicate that the mean SNR in the 60-80 km height range of the GPS L1 signal is over 1500 V/V, with significant numbers of occultations measuring L1 SNRs exceeding 2,000 V/V (Figure 1a). This is much higher than the average

SNR of COSMIC of ~800 V/V. Higher SNR reduces the contribution of thermal noise to bending angle (BA) errors. BA observational errors are commonly characterized by the standard deviation (SD) of retrieved BA from climatology between 60 and 80 km, where the main error contributors are thermal noise, ionospheric residuals, and GNSS clock errors.

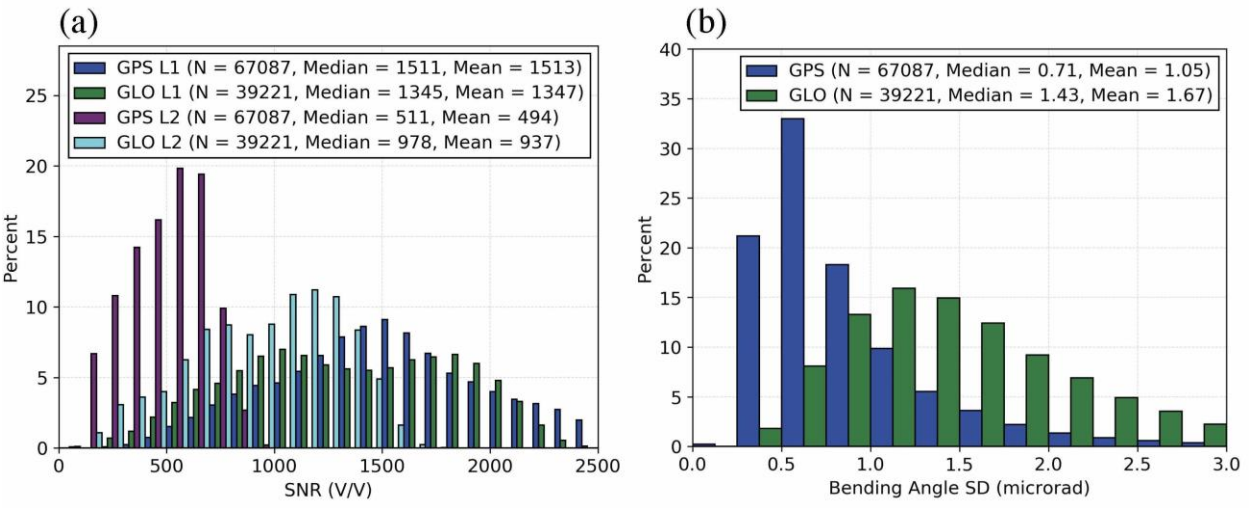

Figure 1: (a) Histograms of SNR for GPS L1 (dark blue) and L2 (purple) and GLONASS L1 (green) and L2 (light blue) signals. (b) Histograms of SD of BA for GPS (blue) and GLONASS (green) occultations. Larger SD for GLONASS is related to larger transmitter clock interpolation errors, which may be reduced by reducing interpolation intervals (currently 30 s for near real-time processing).

High SNR is important in at least three ways: penetration of soundings lower into the troposphere, detection of sharp atmospheric boundary layer (ABL) tops, and detection of super-refraction (SR) on top of the ABL. Figure 2 shows penetration depths above ground level (AGL) for C2 and eight other RO missions for occultations located within 200 km and 2 hours of C2 soundings. While penetration depths depend on the approach used to truncate the retrieved profiles, the use of the same approach for all missions makes the results comparable. As shown in Figure 2a, C2 provides deeper penetration of profiles compared to other RO missions, with 50% reaching within 200 m of the surface. Figure 3(a) shows the penetration depth for C2 occultations over the oceans as function of L1 SNR for GPS and GLONASS, and indicates that higher SNR allows deeper penetration.

Sharp ABL tops can be detected at the heights of maximum BA lapse (BAL, Sokolovskiy et al., 2007). An example is shown in Figure 3(b). Figure 3(c) shows BAL > 0.01 rad as function of L1 SNR. Higher SNR allows retrievals of BA profiles with larger BAL, thus increasing the reliability of detection of sharp ABL tops.

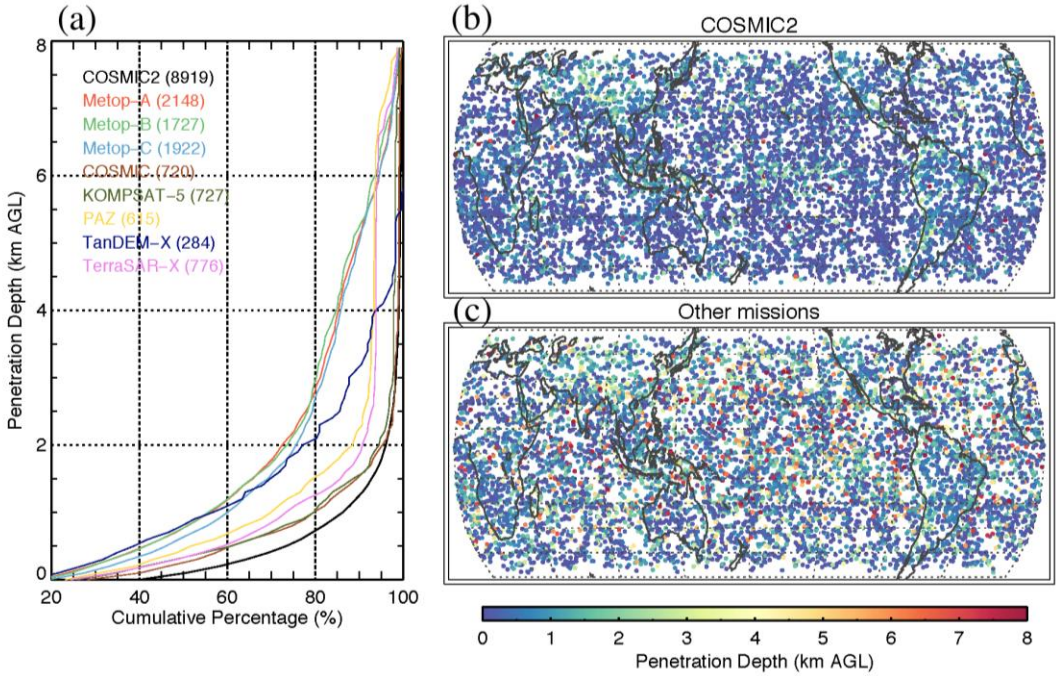

Figure 2: (a) Distributions of the penetration depths (minimal heights AGL of co-located profiles) for C2(black profile) and other RO missions. The number of soundings for each mission is shown in parentheses in the mission labels. Color-coded penetration depths AGL of (b) C2 and (c) other RO missions.

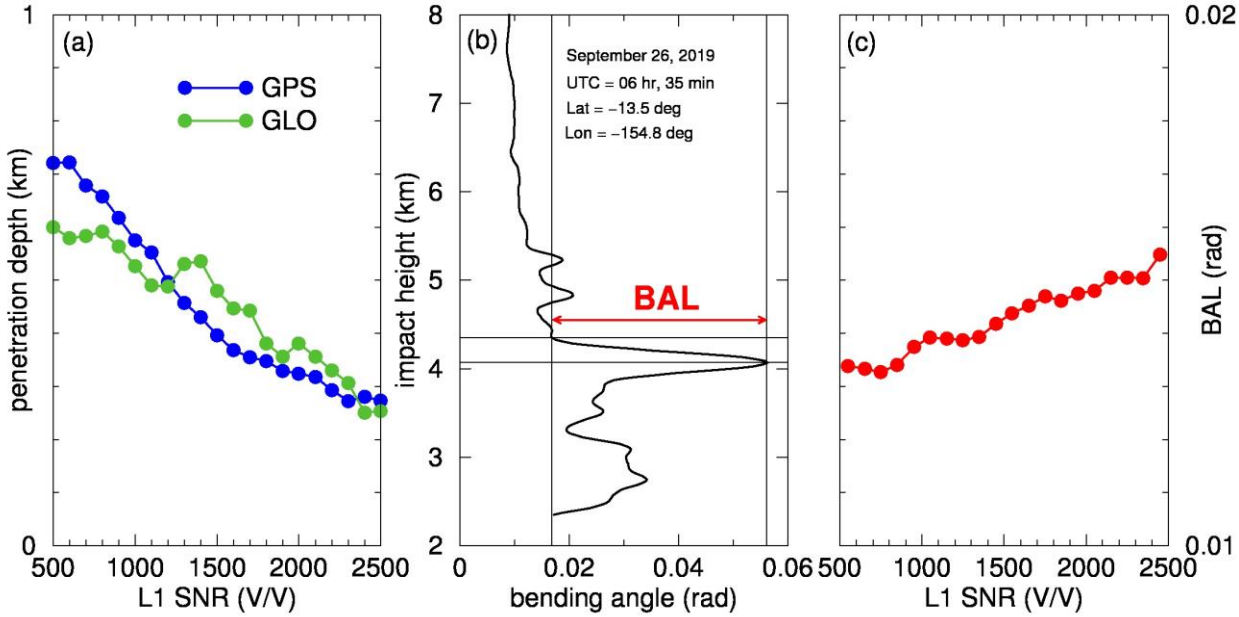

Figure 3: (a) Average C2 penetration depth over the oceans as function of L1 SNR. (b) An example of C2 BA profile with large BAL. (c) Average BAL > 0.01 rad as function of L1 SNR. Panels (a) and (c) represent averaged values in ±100 V/V bins.

SR on top of the ABL is a known problem for RO data assimilation (e.g., Xie et al., 2010). NWP models can reproduce SR, but their predictions may contain errors and so direct observations of SR are useful for NWP as well as weather and climate research. SR can be detected by the existences of very deep signals in spectrograms of RO signals acquired under high SNR (Sokolovskiy et al., 2014). Figure 4 shows three C2 occultations tracked down to -350 km height of straight line transmitter-receiver. Panels (a)-(c) show SNRs. Panels (d)-(f) show spectrograms of RO signals down-converted using a model based on orbit geometry and refractivity climatology (to reduce frequency). Panels (g)-(i) show C2 RO and European for Medium Range Weather Forecasts (ECMWF) BA profiles. All profiles indicate sharp tops of the ABL (the ECMWF profile stops at the height of SR because BA equals infinity at this point). Spectrogram (d) does not show any signal below -150 km, thus no SR, while (e) and (f) show deep signals well below -150 km, thus detecting SR. ECMWF agrees with RO in cases (g) and (h), but not in case (i) where it does not show the SR detected from the RO spectrogram (f).

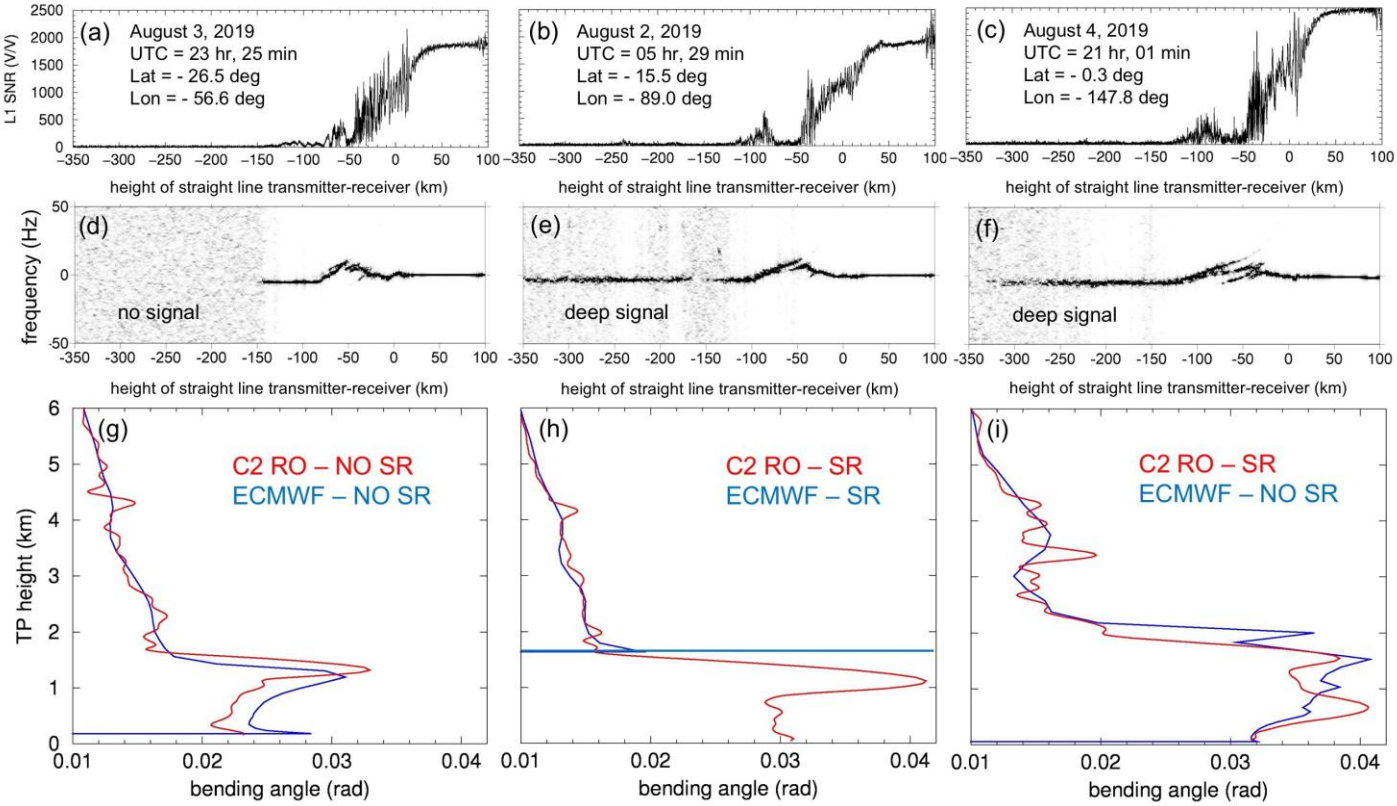

Figure 4: (a)-(c) SNRs for three C2 occultations. (d)-(f) spectrograms of RO signals down-converted using frequency model (see text). (g)-(i) BA as functions of tangent point (TP) height for C2 RO (red) and ECMWF (blue).

2.2. Precision estimates from intra-comparison of C2 satellite data

Following launch, the C2 satellites were located close together for a short period of time, enabling estimation of the precision of the BA retrievals by comparing the BA from two nearby satellites at nearly the same time with similar occultation geometry. Figure 5 shows the mean and SD of the differences of 265 pairs of quality-controlled C2 soundings (GPS and GLONASS) with horizontal separations of tangent points < 20 km from 16 July to 4 September 2019 between 10 km and 60 km altitude. There is a very small bias and a SD of approximately 2.2 microradians between 30 and 60 km and less than about 30.0 microradians between 10 and 30 km. Under the assumption that paired soundings have uncorrelated errors of the same magnitudes, the random uncertainty of individual sounding (the precision) is estimated to be the SD divided by the square root of two. This results in a precision estimate of ~1.6 microradians for the 30-60 km altitude range, which is well below the C2 mission requirement value of 2.0 microradians.

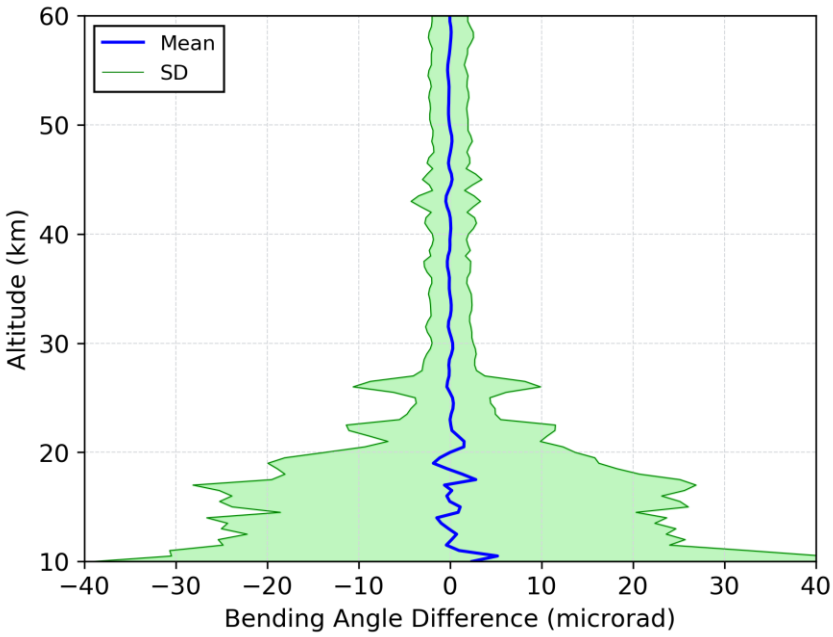

Figure 5: Mean and SD of BA differences from 265 pairs of nearby C2 satellites between 10 and 60 km.

2.3. Comparison with other data sets

We compared the October 2019 C2 data set with operational radiosondes (RS), short-term forecasts from the National Centers for Environmental Prediction (NCEP) and ECMWF) forecast models, and the MERRA-2 reanalysis. Figure 6 shows the mean and SD of the differences between the BA and refractivity profiles from C2 and from co-located ECMWF operational short-term forecasts. Both the GPS and GLONASS retrievals are consistent with each other and show very little bias compared to ECMWF in the altitude range 2 to 40 km and negative biases below 2 km. RO biases in the lower troposphere are known to be caused by a combination of different factors: SR (affects refractivity; Ao et al., 2003; Sokolovskiy, 2003; Xie et a., 2006; Ao, 2007; Xie et al., 2010), tracking depth and noise (Sokolovskiy, 2003; Sokolovskiy et al., 2010), and fluctuations of refractivity (Gorbunov et al., 2015; Gorbunov and Kirchengast 2018). Analysis of RO biases, their dependence on the processing and the SNR is complicated and is the subject of separate study. The increased SD at ~19-25km for GPS is thought to be associated with technical problems of tracking L2P signals, and is expected to be resolved in the future.

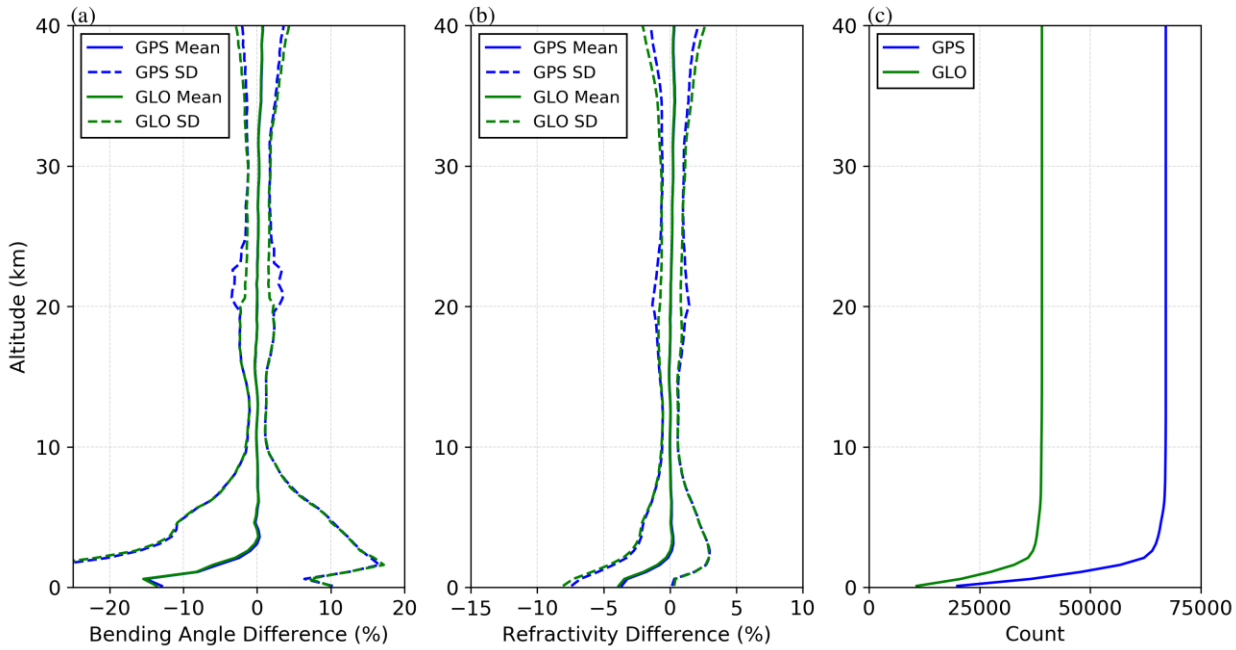

Figure 6: (a) Mean and SD of differences in BA between C2 and ECMWF from GPS (blue) and GLONASS (green) occultations. (b) Same as left panel except for refractivity. (c) Counts of GPS (blue) and GLONASS (green) occultations.

The three-cornered hat (3CH) method (Anthes and Rieckh, 2018, hereafter AR2018; Rieckh and Anthes, 2018) is used to estimate the random error SD (uncertainty) of the C2 refractivity observations using four other data sets (listed in caption of Fig. 7). The model data sets are interpolated to the locations, times, and mandatory levels of the operational radiosondes (RS), while RO data within 3h and 300 km of the RS locations are interpolated in the vertical to the RS mandatory levels. The 3CH equations include the bias correction terms, which remove biases among the data sets (O'Carroll et al., 2008). The major limitation of the 3CH method, the potential correlation of errors between the four data sets and C2, is expected to be small since the October 2019 C2 data were not assimilated in any of the models or reanalyses.

Figure 7 shows the 3CH results for the five data sets. Five data sets produce six independent 3CH estimates of the error SD. For these data sets the ECMWF and NCEP GFS (Global Forecast System) analyses show the smallest SD of errors, while the RS show the largest SD, mainly due to representativeness errors as found by AR2018. The C2 and MERRA2 error SD are in the middle. The C2 random errors are similar to those of COSMIC (AR2018) as expected. Also shown in Figure 7 are the mean and SD of the differences between C2 and each of the other four data sets. The mean and SD of differences between two data sets is a common method of comparing the random errors of different data sets. As shown in Figure 7, the 3CH estimates of the RO error SD are always less than the SD of the difference between RO and the other data sets.

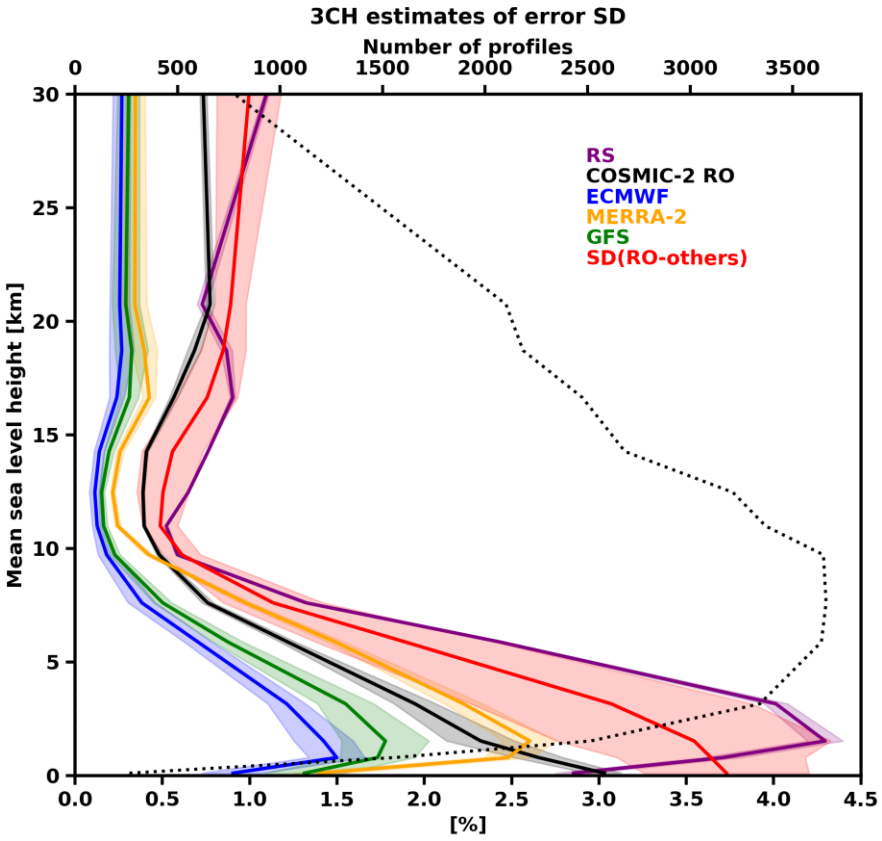

Figure 7: 3CH estimates of refractivity error SD of COSMIC-2 (black), ECMWF analysis (blue), NCEP GFS analysis (green), MERRA-2 reanalysis (orange) and radiosondes (purple). The mean of the six SD estimates for each data set are the solid lines and the SD around this mean is indicated by the shading. Also shown is the mean SD of differences between C2 and each of the other four data sets (red) and the SD around this mean (red shading).

3. Conclusions

Early results from the COSMIC-2 mission indicate that the stratospheric and tropospheric profiles of radio occultation bending angle and refractivity are meeting their high expectations. The mean and median SNR values are higher than any previous radio occultation mission, which enables deeper tropospheric penetration (50% within 200 m of Earth's surface) of the soundings. The higher SNR also enables better observation of the atmospheric boundary layer depth and detection of super-refraction on top of the atmospheric boundary layer.

Comparison of bending angle profiles from nearby COSMIC-2 satellites shortly after launch demonstrates high precision and low bias of the data. Comparison of over 100,000 COSMIC-2 vertical profiles of bending angles and refractivities from October 2019 with other independent data sets, including radiosondes, short-term operational forecasts, and the MERRA-2 reanalyses shows very small biases from about 2 km to 40 km. Random error profiles of COSMIC-2 refractivity are generally less in magnitude than radiosondes and the MERRA-2 reanalysis in the troposphere, but higher than the short-term forecasts. In the stratosphere, the COSMIC-2 and radiosonde errors are comparable, and greater than those of the model data sets.

These results indicate that high-SNR COSMIC-2 radio occultation soundings open up exciting new opportunities to study the challenging tropical atmosphere, will significantly benefit operational NWP forecasts, and will provide valuable data of unprecedented quality that are freely available to the international scientific community.

Acknowledgments and Data Availability

COSMIC-2 is a partnership between the National Space Organization in Taiwan and NOAA, the U.S. Air Force, and the University Corporation for Atmospheric Research (UCAR) in the United States. The UCAR work is sponsored by NSF-NASA grant 1522830, NOAA Contract 16CN0070, Air Force contract 319C004 and NSPO-UCAR AIT-TECRO Agreement Implementing Arrangement #5.

All data used in this paper are available from the UCAR COSMIC Data Analysis and Archive Center (www.cosmic.ucar.edu). Please contact the corresponding author for details on access.

References

Anthes, R.A. and T. Rieckh (2018). Estimating observation and model error variances using multiple data sets. *Atmos. Meas. Tech.*, 11, 4239–4260, 2018. https://doi.org/10.5194/amt-11-4239-2018

Anthes, R. and W. Schreiner (2019). Six new satellites watch the atmosphere over Earth's Equator. *Eos*, **100**, https://doi.org/10.1029/2019EO131779.

Ao, C. O., T. K. Meehan, G. A. Hajj, A. J. Mannucci, and G. Beyerle (2003). Lower troposphere refractivity bias in GPS occultation retrievals, *J. Geophys. Res.*, **108** (D18), 4577, https://doi.org/10.1029/2002JD003216

Ao, C. O. (2007). Effect of ducting on radio occultation measurements: An assessment based on high-resolution radiosonde soundings, *Radio Sci.*, **42**, RS2008, doi:10.1029/2006RS003485

Gelaro, R., W. McCarty, M.J. Suarez, R. Todling, A. Molod, L. Takacs, C.A. Randlesm, A. Darmenov, M.G. Bosilovich, R. Reichle, K. Wargan, L. Coy, R. Cullather, C. Draper, S. Akella, V. Buchard, A. Conaty, A. M. Da Silva, W. Gu, G.-K. Kim, R. Koster, R. Lucchesi, D. Merkova, J.E. Nielsen, G. Partyka, S. Pawson, W. Putman, M. Rienecker, S.D. Schubert, M. Sienkiewicz and B. Zhao (2017). The Modern-Era Retrospective Analysis for Research and Applications, Version 2 (MERRA-2). *J. Climate*, **30**, 5419-5454, DOI: 10.1175/JCLI-D-16-0758.1.

Gorbunov, M. E., V. V. Vorob'ev and K. B. Lauritsen (2015). Fluctuations of refractivity as a systematic error source in radio occultations, *Radio Sci*., **50**, 656-669, doi:10.1002/2014RS005639.

Gorbunov, M. E. and G. Kirchengast (2018). Wave-optics uncertainty propagation and regression-based bias model in GNSS radio occultation bending angle retrievals, *Atmos. Meas. Tech*., 11, 11-125, doi:10.5194/amt-11-11-2018.

Ho, S.-P., R.A. Anthes, C.O. Ao, S. Healy, A. Horanyi, D. Hunt, A.J. Mannucci, N. Pedatella, W.J. Randel, A. Simmons, A. Steiner, F. Xie, X. Yue, and Z. Zeng, 2019. The COSMIC-FORMOSAT-3 radio occultation mission after 12 years: accomplishments, remaining challenges, and potential impacts of COSMIC-2 (2019). *Bull. Am. Meteorol. Soc*., **100**, online version: https://journals.ametsoc.org/doi/pdf/10.1175/BAMS-D-18-0290.1

O'Carroll, A.G., J.R. Eyre, and R.S. Saunders (2008). Three-way error analysis between AATSR, AMSR-E, and in situ sea surface temperature observations. *J. Atmos. Oceanic Tech*., **25**,1197-1207, doi:10.1175/2007JTECHO542.1.

Rieckh, T. and R.A. Anthes (2018): Evaluating two methods of estimating error variances using simulated data sets with known errors. *Atmos. Meas. Tech*., **11**, 4309-4325, https://doi.org/10.5194/amt-11-4309-2018

Sokolovskiy, S. (2003). Effect of superrefraction on inversions of radio occultation signals in the lower troposphere, *Radio Sci*., **38**, 1058, doi:10.1029/2002RS002728.

Sokolovskiy, S. V., C. Rocken, D. H. Lenschow, Y.-H. Kuo, R. A. Anthes, W. S. Schreiner and D. C. Hunt (2007). Observing the moist troposphere with radio occultation signals from COSMIC. Geophys. Res. Lett., **34**, https://doi.org/10.1029/2007GL030458.

Sokolovskiy, S., W. Schreiner, Z. Zeng, D. Hunt, Y-C-Lin, and Y.-H. Kuo (2014). Observation, analysis, and modeling of deep radio occultation signals. Effect of tropospheric ducts and interfering signals. *Radio Sci*., **49**, doi:10.1002/2014RS005436.

Tien, J.Y., Okihiro, B. Bachman, Esterhuizen, S.X., Franklin, G.W., Meehan, T.K., Munson, T.N., Robison, D.E., Turbiner, D., Young, L.E. (2012). "Next Generation Scalable Spaceborne GNSS Science Receiver," *Proceedings of the 2012 International Technical Meeting of The Institute of Navigation*, Newport Beach, CA, January 2012, pp. 882-914.

Xie, F., S. Syndergaard, E. R. Kursinski, and B. M. Herman (2006). An approach for retrieving marine boundary layer refractivity from GPS radio occultation data in the presence of super-refraction. *J. Atmos. Oceanic Technol.*, **23**, 1629–1644, https://doi.org/10.1175/JTECH1996.1

Xie, F., D.L. Wu, C. O. Ao, E. R. Kursinski, A. J. Mannucci and S. Syndergaard (2010). Super-refraction effects on GPS radio occultation refractivity in marine boundary layers. *Geophys. Res. Lett*., **37**, https://doi.org/10.1029/2010GL043299.